Mol. Cryst. Liq. Cryst., 1987, Vol. 151, pp. 47-68
Photocopying permitted by license only

Printed in the United States of America

PROPERTIES OF A HOMOLOGOUS SERIES OF FERROELECTRIC LIQUID CRYSTALS

L.BATA, A.BUKA, N.ÉBER, A.JÁKLI, K.PINTÉR, J.SZABON and A.VAJDA
Central Research Institute for Physics
H-1525 Budapest 114, P.O.B.49. Hungary

Abstract A homologous series of MBOPEnOBA chiral compounds has been synthesized and some chemical and physical properties of the components as well as that of a binary mixture has been studied. Measurements of the spontaneous polarization and the pitch are presented and results of eutectic, dielectric, electrooptic and electromechanical investigations are given.

INTRODUCTION

Considerable attention has been paid to chiral smectic C* (S_C^*) liquid crystals because of their fundamental and practical interest.[1] In this paper we present details on some compounds and a binary mixture which exhibit this phase and we describe some physical and chemical properties such as spontaneous polarization, pitch, eutectic, dielectric, electrooptic and electromechanical properties of these compounds. For both fundamental research and practical application it is a great advantage if the compound possesses S_C^* phase at room temperature so our first task was to produce such compounds.

COMPOUNDS

The general structure of the 4-(2'-methylbutyloxy)-phenyl-4-alkyloxy-benzoate homologues (MBOPEnOBA) is as follows (n=8 to 12)

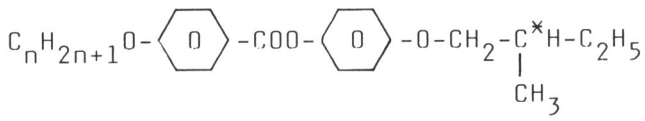

(The asymmetric centre is marked with an asterisk.) The types of mesomorphic phases and the phase transition temperatures of these compounds are listed in Table I.

TABLE I Mesomorphic phases of MBOPEnOBA

	n	Cr_3	Cr_2	Cr_1	S_C^*	S_A	Ch	I
A	8	24.8§	36.8§	39.5§	(37)	54	67	
	9	-	44	-	(42)	58	60	
	10	-	44	-	47	65	67	
	11	-	46	-	49	65	-	
B	12	-	44.1§	46.1§	(46)	66	-	

The transition temperatures are given in °C
( ) monotropic transitions
n number of C atoms in alkyloxy chain
§ Calorymetric data

The phase transition temperatures of the A compound are somewhat different from the data published earlier.[2] We explain the differences with the presence of an intermedier substance which apart from affecting the phase transition temperatures

extends the range of the cholesteric phase.

The phase transition temperatures were determined by a universal polarizing microscope (Zeiss Amplival) equipped with a heating stage. It was observed that none of the compounds has the chiral S_C^* phase at room temperature therefore the binary mixtures of the compounds were also investigated. The most interesting phase diagram is shown in Fig.1. The mixture, called Fk4, containing 60% by weight of the compound with n=8, i.e. compound (A), and 40% by weight of n=12, i.e. compound (B), exhibits the S_C^* phase around room temperature so this mixture was chosen for further investigation. (The mixture with 80% of component A shows solidification

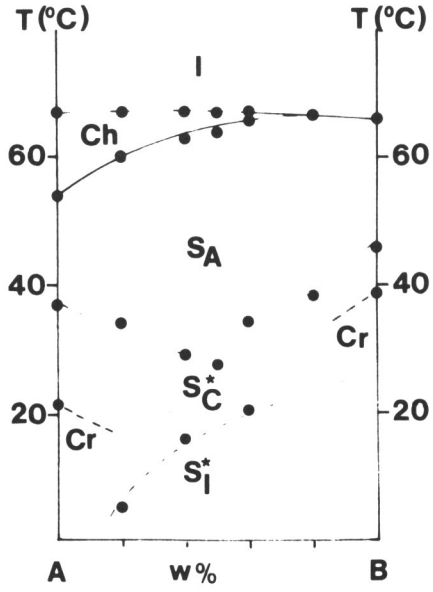

FIGURE 1. Phase diagram of MBOPE8OBA and MBOPE12OBA mixture

at room temperature). The phase sequence of Fk4 compounds reads

$$S_I^* \xleftrightarrow{16^oC} S_C^* \xleftrightarrow{29^oC} S_A \xleftrightarrow{63^oC} Ch \xleftrightarrow{67^oC} I$$

Here the standard notation was used.

PITCH AND SPONTANEOUS POLARIZATION

In addition to the appropriate temperature interval the pitch and the spontaneous polarization are the most important material characteristics of S_C^* substance.

The pitch can be measured by observing the stripe structure with an ocular micrometer attached to the polarizing microscope[3]. Either nonoriented samples with a fan-shaped texture, (Fig.2a) or planar oriented cells (Fig.2b) can be used for

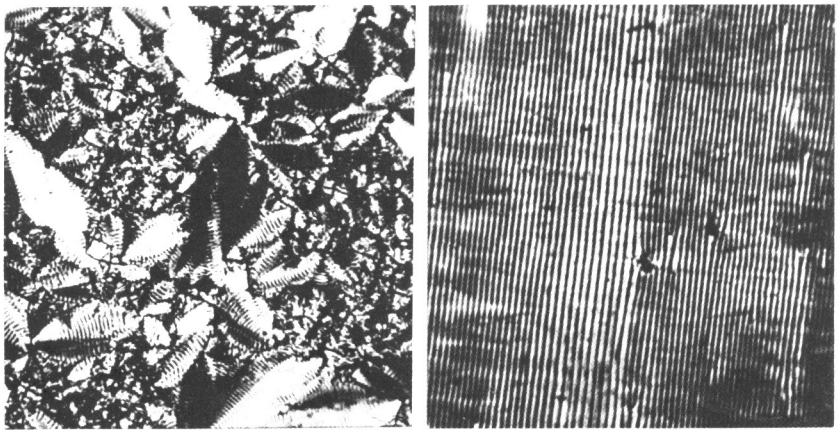

a. fan-shaped b. planar

Figure 2. Textures of the Fk4 mixture in the S_C^* phase.

this purpose. In the case of the Fk4 mixture the pitch is approximately 5 μm at T=23^{o}C.

In order to measure spontaneous polarization one has to prepare a planar oriented sample (smectic layers are perpendicular to the bounding surfaces). We oriented the sample by the shear method[4] which yields good quality alignment (Fig.2b).
The spontaneous polarization was determined from the P-E hysteresis loop. A typical experimental curve is shown in Fig.3.
Our loop tracer[5] consisted of a Diamant bridge[6] which is connected to a microcomputer allowing measurements at low frequencies (1-10 Hz). The temperature dependence of the spontaneous polarization of the Fk4 mixture is shown in Fig.4. It reaches a maximum value of $P_s = 1.6 \times 10^{-5} \frac{C}{m^2}$ at T=19^{o}C. Similar values were found for some members of the

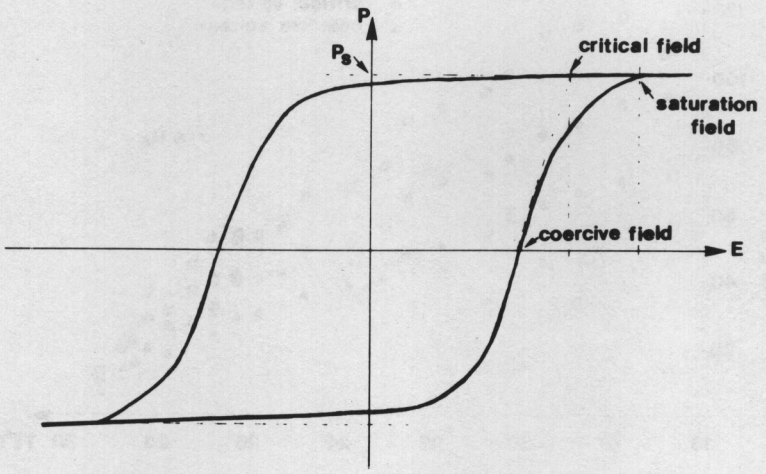

FIGURE 3. Typical hysteresis curve.

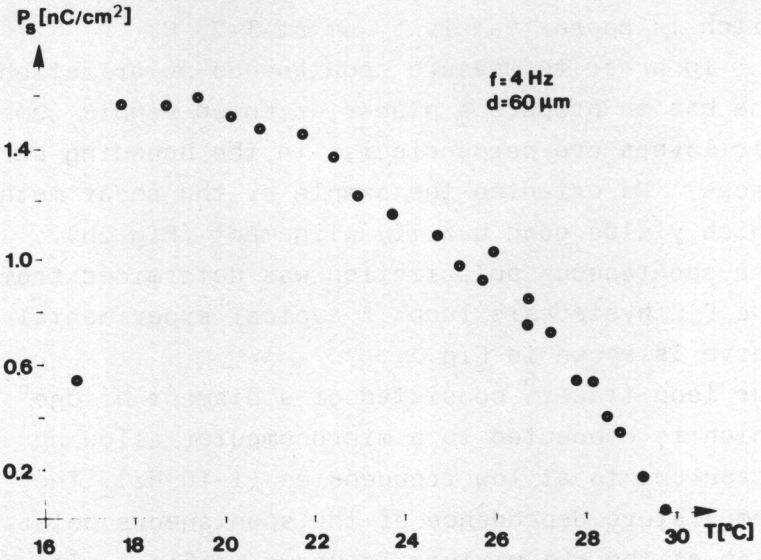

FIGURE 4. Temperature dependence of the spontaneous polarization of the Fk4 mixture.

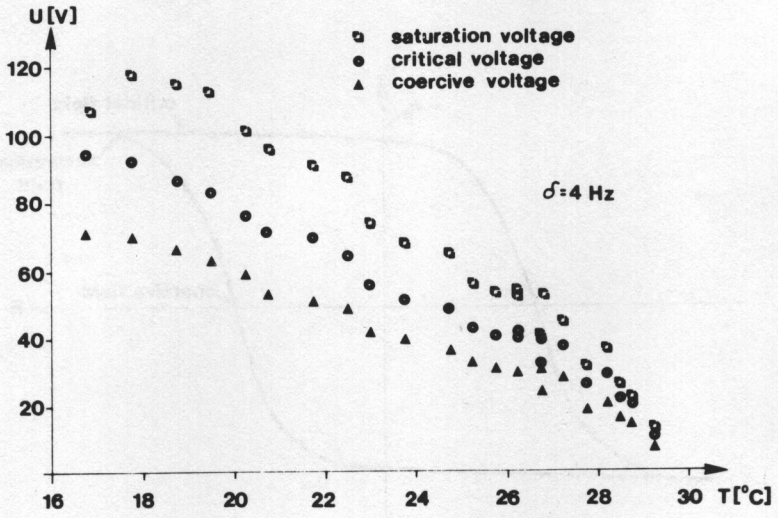

FIGURE 5. Temperature dependence of coercive, critical and saturation voltages of a 60 µm thick Fk4 sample.

same homologous series[7]. It is worth noticing that the measured values of the spontaneous polarization depend strongly on the quality of the planar orientation of the cell. Any deterioration of the alignment leads to an effective decrease of the polarization.

From the hysteresis curves which are similar to that in Fig.3 the coercive U_c, the critical U_{cr}, and the saturation U_s voltages were determined for a 60 μm thick sample. Each parameter shows a marked increase with decreasing temperature (Fig.5).

DIELECTRIC PERMITTIVITY

Experiments have been carried out on 1 mm thick aligned samples of the n=10 member of the homologous series (see above) as well as on the binary mixture Fk4. Orientation was established by slow cooling of the sample in a magnetic field of $\sim$1T, from the isotropic to the S_A phase. Further cooling through the T_{AC}^* point was carried out with no magnetic field.

Static dielectric permittivity data are shown in Figs. 6 and 7 for the one-component system and the binary mixture respectively. Points are given for all phases observed in two directions, viz. parallel and perpendicular to the magnetic field. Data are well reproducible for both directions in the S_C^* phase also, where $\parallel$ labels the direction along the smectic layer normal while $\perp$ lies within the layer.

The dielectric anisotropy is negative for both

samples and the temperature behaviour of both $\varepsilon_\perp$ and $\varepsilon_\parallel$ shows no anomaly around the phase transitions for 5 kHz, which is the usual frequency for the static permittivity measurements[8].

Figure 7 shows points measured at 20 Hz around $T_{AC}*$ for the perpendicular alignment. The difference in S_A between $\varepsilon_\perp$(5kHz) and $\varepsilon_\perp$(20 Hz) can be explained by the conductivity effect. The deviation

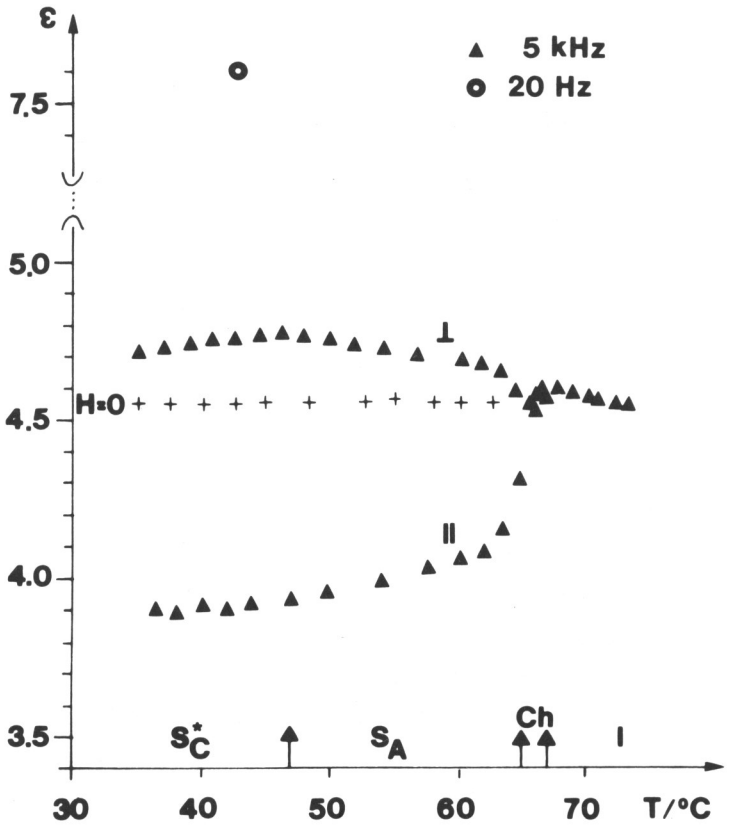

FIGURE 6. Static dielectric permittivity for MBOPE100BA

decreases with decreasing temperature. The strong increase of $\varepsilon_{\perp}$(20 Hz) at $T_{AC}*$ is connected[9] with the appearance of the new dielectric mode (Goldstone mode) in the ferroelectric phase.

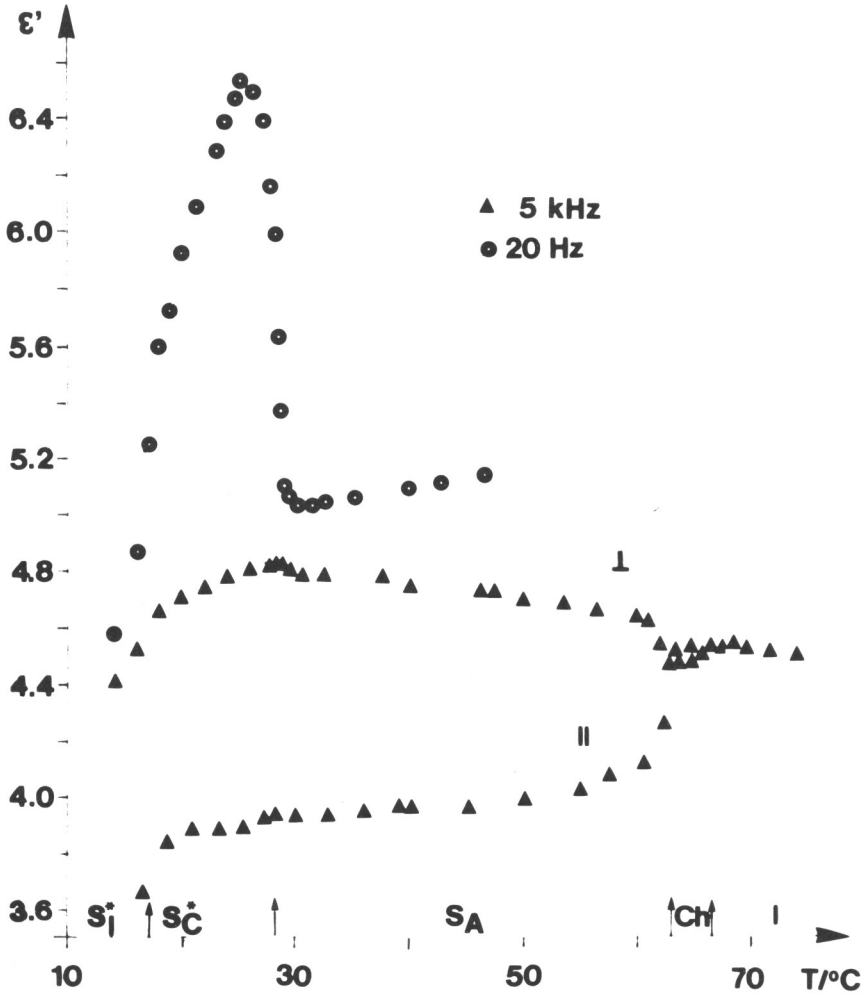

FIGURE 7. Static dielectric permittivity for Fk4 mixture

Dispersion measurements were carried out for all observed phases in both alignments in the frequency range 20 Hz - 100 kHz. The parallel orientation exhibited dispersion connected with the rotational diffusion of the molecules around their short axis was found. The dispersion is of Debye type. Arrhenius plots of critical frequencies are shown in Figs.8 and 9 for S_A, S_C^* and S_I^* phases. In Fig.9, at the S_C^* - S_I^* phase transition, f_c exhibits a change of about one order of magnitude, representing a similar behaviour to the one found earlier[8] for nonchiral substances that exhibited a transition from a two-dimensional liquid type smectic structure (S_A or S_C) to a hexagonally ordered layer

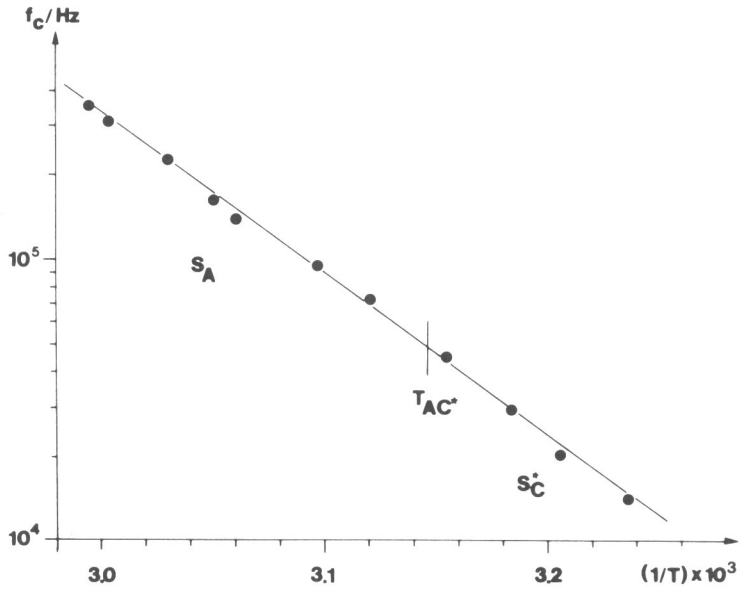

FIGURE 8. Arrhenius plot of the critical frequency for the parallel alignment of MBOPE100BA.

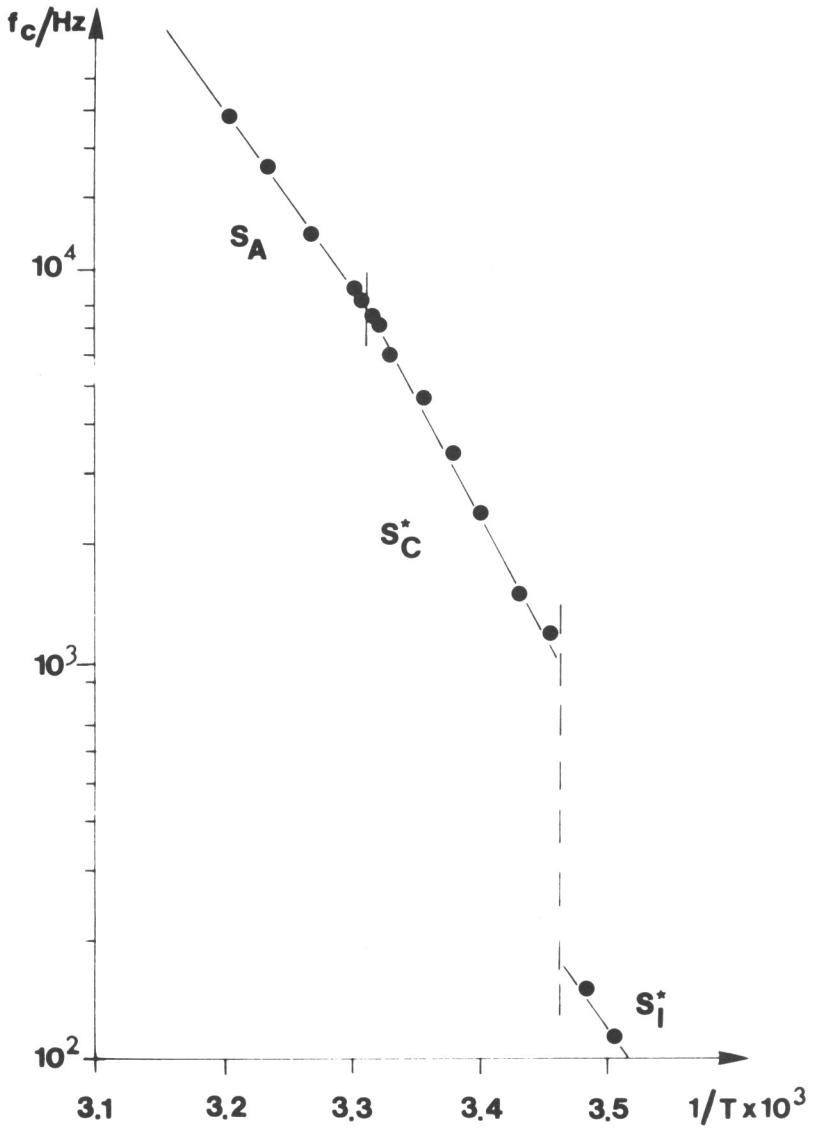

FIGURE 9. Arrhenius plot of critical frequency for the parallel alignment of Fk4 mixture.

system (S_B or S_I).

The frequency dependence of the permittivity in the perpendicular alignment of the Fk4 binary mixture is demonstrated in Fig. 10a,b. Figure 10 a shows the imaginary part of the permittivity versus frequency in the cholesteric and smectic A phases of the binary mixture. No significant dispersions were found in these two phases.

The general expression for the frequency dependence of the dielectric loss $\varepsilon''(f)$ is[10]:

$$\varepsilon''(f)=\frac{G}{2\pi f C_o}+(\varepsilon_o-\varepsilon_\infty)\frac{1}{1+\frac{f^2}{f_c^2}}\frac{f}{f_c} \qquad (1)$$

where: G - conductivity

C_o - geometric capacity

$(\varepsilon_o-\varepsilon_\infty)$ - dielectric increment

f_c - critical frequency of a Debye type dispersion.

When $f \ll f_c$ (for frequencies far below the dispersion region) the dielectric loss has a pure conductivity character:

$$\log \varepsilon'' = \log \frac{G}{2\pi C_o} - \log f \qquad (2)$$

and we get a straight line for a log ε''(logf) plot with a slope of -1 which is exactly the case for Fig.10 a.

The dielectric loss versus frequency for the S_C^* and S_I^* phases of the Fk4 compound can be seen in Fig.10 b. In the 10^3- 10^5Hz region of the $\varepsilon_\perp''$

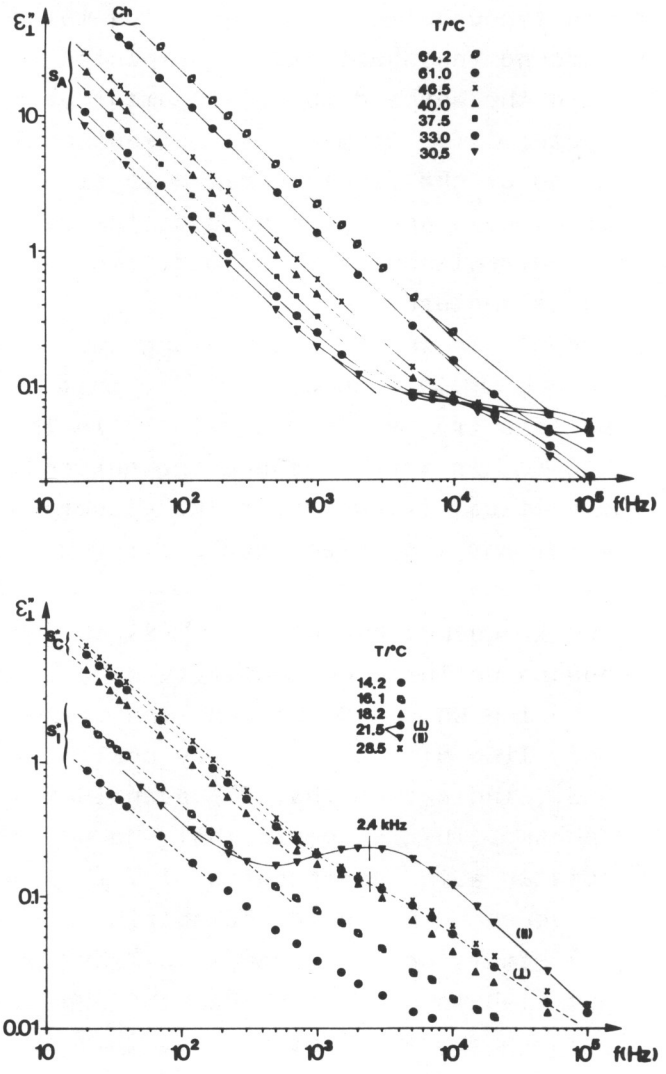

FIGURE 10. Dielectric loss versus frequency in the perpendicular alignment of Fk4.
a. Ch and S_A phases
b. S_C^* and S_I^* phases, (∥) corresponds to a parallel alignment measurement

curves one can see the influence of the dispersion recorded in the parallel alignment. The molecular rotation around the short axis is expected to have an effect in the perpendicular alignment of tilted, biaxial systems[8] for geometrical reasons, as long as the direction of the electric field in either alignment ($\parallel$ or $\perp$) does not correspond to the easy directions (main directions of the dielectric tensor) of the biaxial structure.

To demonstrate this effect, among the perpendicular curves Fig.10b shows one $\varepsilon''_{\parallel}$, that is the continuous line ($\parallel$) measured at 21.5°C in the S_C^* phase. Line ($\perp$) is the corresponding perpendicular plot. The critical frequency of the dispersion for $\varepsilon_{\parallel}$ is 2.4 kHz and its effect can clearly be seen on curve $\parallel$.

The low frequency end of the $\varepsilon''_{\perp}(f)$ curves in Fig.10 shows a definite conductivity behaviour similarly to the Ch and S_A phases. The slope of the log $\varepsilon''_{\perp}$(logf) line did not change by cooling from S_A to S_C^* and S_I^*, indicating that $\varepsilon''_{\perp} \sim \frac{1}{f}$ even in the ferroelectric phases. This suggests that the Goldstone mode associated with the increase of $\varepsilon'_{\perp}$ with decreasing frequency in the ferroelectric phases (see Fig.7) cannot be described by a Debye process. Although we wish to emphasize that the expected effect in $\varepsilon''_{\perp}$ (which is about half of that found for $\varepsilon'_{\perp}$) is rather small, even so it should still be seen in Fig. 10 at least as an increase in the slope of the lines.

The same conclusions could be drawn from the frequency dependence of the perpendicular permit-

tivity of the single component system.

ELECTROOPTICAL RESPONSE

Unwinding threshold voltage

In the absence of electric field a thick planar oriented S_C^* sample exhibits a stripe structure as observed between crossed polarizers under the microscope (Fig.2b). If a large enough DC or AC electric voltage is applied to the sample the stripes disappears, the helix unwinds and a uniformly aligned planar S_C texture results[11]. Figure 11. shows the frequency dependence of the unwinding threshold amplitude U_{th} of the sine-shaped AC voltage for the Fk4 mixture at T=24°C. Below 1 Hz there is only a slight difference between the DC thresh-

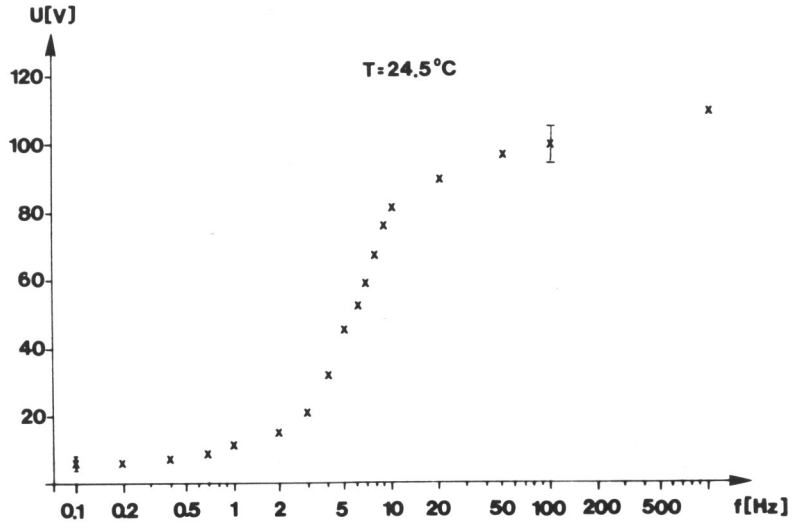

FIGURE 11. Frequency dependence of the unwinding threshold voltage for a 60 /um thick Fk4 sample.

old and AC threshold which grows up around $f_c \approx 7$ Hz and goes to a saturation at high frequencies.[12] This behaviour may be due to the different unwinding mechanisms in the low and high frequency regions.[13] It is also worth mentioning that at low frequencies the stripes can reappear during each period when the momentary value of the AC voltage decreases below the threshold value.

In Fig.12 a comparison is given between the

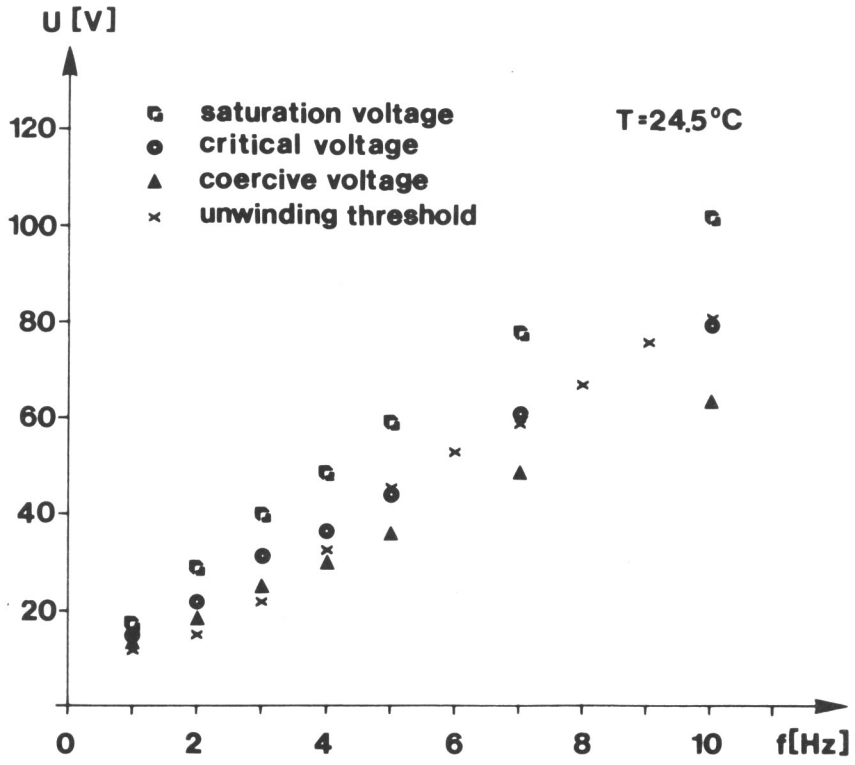

FIGURE 12. Frequency dependence of the unwinding threshold, coercive, critical and saturation voltages for a 60 μm thick Fk4 sample.

unwinding threshold voltage U_{th} and the coercive U_c, critical U_{cr} and saturation U_s ones. It can be seen that the U_{th}, which was measured by the microscope, essentially corresponds to U_{cr} determined from the hysteresis loop (c.Fig.3).

Switching time

If a bipolar square wave shaped voltage is applied to the planar oriented S_C^* sample there will be a periodic switching between two states supposing that the amplitude of the applied voltage is higher than the unwinding threshold. Both states have homogeneous textures which can be characterized by the spontaneous polarization pointing up and down respectively throughout the sample. If the cell is placed between crossed polarizers and is illuminated by a laser beam, the transmitted intensity changes according to the switching which can be monitored by a photodiode allowing the measurement of the switching times.

We applied a symmetrical bipolar square wave to the sample and found that the switching time at the rising and falling edges are equal. This indicates that in the absence of electric field there is a symmetrical antiparallel molecular alignment at the bounding plates. Figure 13 shows the temperature dependence of the switching time for a 60 /um thick Fk4 sample using an applied electric field $E=10^6 \frac{V}{m}$. τ increases by about an order of magnitude while the temperature decreases from $T_{AC}=29^oC$ to $T_{CI}=16^oC$. For a large electric field the switching time τ can be approximated by the expression $\tau = \frac{\eta}{P_s E}$ where η

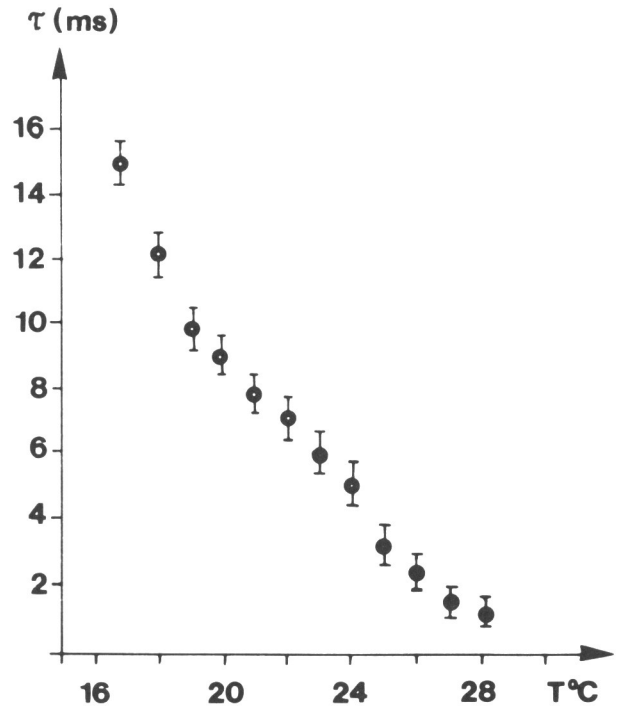

FIGURE 13. Temperature dependence of the switching times for a 60 /um thick Fk4 sample

is the orientational viscosity and P_s is the spontaneous polarization.[1] Using this expression we can combine Figs.13 and 4 to calculate the orientational viscosity coefficient. As can be seen in Fig.14, η increases by about an order of magnitude when cooling down through the S_C^* phase. Plotting $\ln\eta$ against $\frac{1}{T}$ one can see that it can be approximated by a linear relationship except in the neighbourhood of the $S_A \leftrightarrow S_C^*$ phase transition. It suggests that the rotation of the director around the helical axis may be a thermally activated process, however the situation is more complicated near the

phase transition.

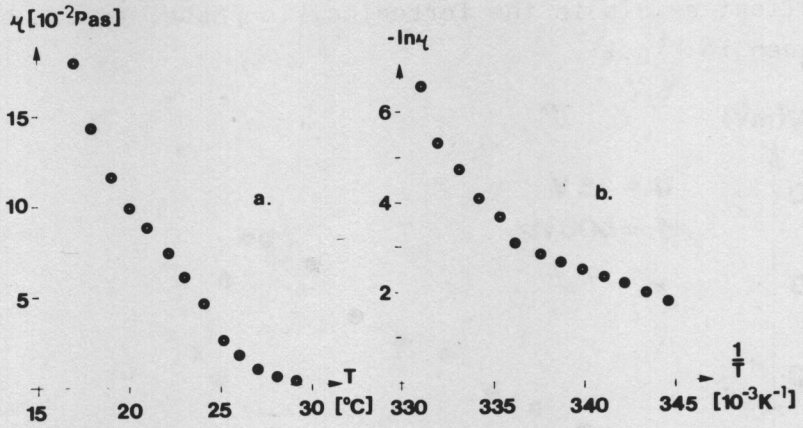

FIGURE 14. Temperature dependence of the orientational viscosity coefficient.
a. $\eta(T)$ curve, b. $\ln\eta(\frac{1}{T})$ curve

ELECTROMECHANICAL PROPERTIES

As we have already mentioned these materials exhibit an electromechanical effect in the S_C^* phase.[14] In our experimental set-up one of the plates of the planar oriented sandwich cell is connected to the membrane of a loudspeaker. Under the influence of an AC electric field this plate oscillates in a direction perpendicular to both the field and the helical axis. The frequency of the oscillation equals that of the applied field, and the amplitude of the displacement as measured by a ceramic pick-up is proportional to both the amplitude and the frequency of the field if $f \lesssim 300$ Hz. This indicates that the effect is linear. In a 10 μm thick Fk4 sample we could detect a maximum vibrational amplitude of

about 5 /um at f=750 Hz and U=25 V. We should like to emphasize that the linear electromechanical effect exists in the ferroelectric phase, as can be seen in Fig.15.

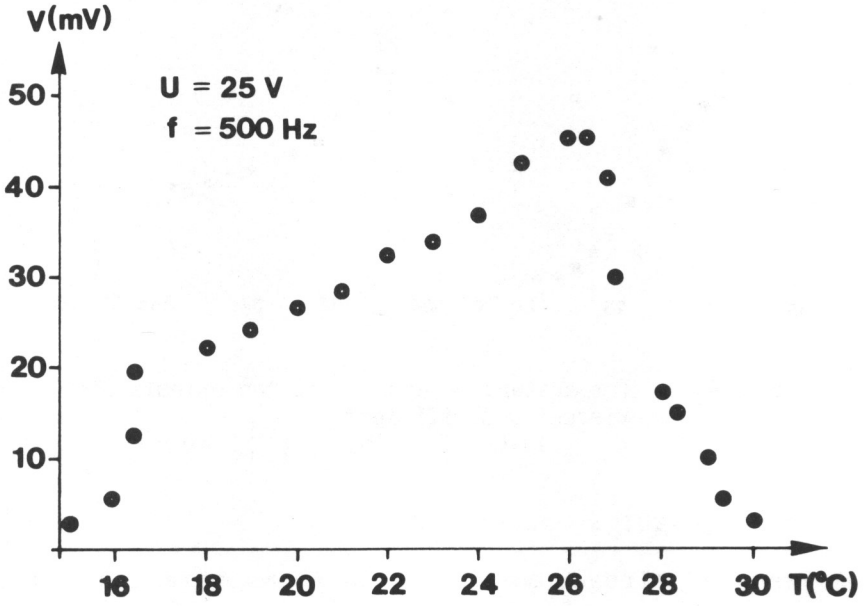

FIGURE 15. Temperature dependence of the electromechanical effect. V is proportional to the displacement

In this paper we should like to draw attention to the inverse electromechanical effect which has also been observed. When a planar oriented S_C^* sample is subjected to a shear flow by moving the plates relative to each other in a direction parallel to the smectic layers, an electric voltage can be detected on the electrodes (Fig.16). Such a shear

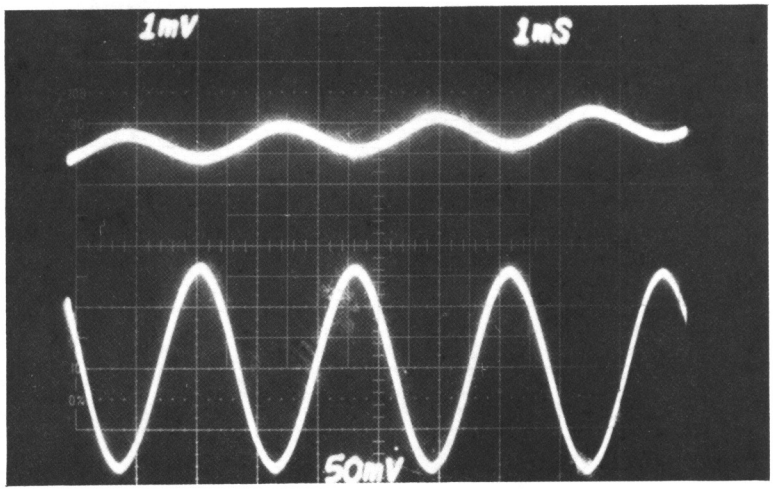

FIGURE 16. Inverse electromechanical effect in planar Fk4 sample. Lower curve corresponds to the shear, the upper one to the detected voltage

induced polarization has previously been observed only in homeotropic S_C^* samples.[15]

REFERENCES

1. N.A. Clark, M.A. Handschy, S.T. Lagerwall, Mol.Cryst.Liq.Cryst, 94, 213 (1983)
N.A. Clark, S.T. Lagerwall, Appl.Phys.Lett., 36, 899 (1980)
2. P. Keller, Ferroelectrics, 58, 3 (1984)
K. Sharp and G. Andersson, Ferroelctrics Lett., 6, 67 (1986)
K. Furukawa, private communication
3. K. Kondo, A. Fukuda, E. Kure, Japan J.Appl. Phys., 20, 1779 (1981)
Ph. Martinot-Lagarde, J.Physique, 37, C3-129 (1976)
4. A. Jákli, L. Bata, Á. Buka, N. Éber, Patent Applied for.
5. L. Bata, N. Éber, Hung.Patent, 190.296

6. H. Diamant, K. Drenck, R. Pepinsky, Rev.Sci. Instrum., 28, 30 (1957).
7. B.I. Ostrovskii, A.Z. Rabinovich, A.S. Sonin, E.L. Sorkin, Ferroelectrics, 24, 309 (1980).
8. L. Bata and Á. Buka, Mol.Cryst.Liq.Cryst., 135, 49 (1986).
Á. Buka, L. Bata, K. Pintér, J. Szabon, Mol. Cryst.Liq.Cryst.Lett., 72, 285 (1982).
9. A. Levstik, B. Zeks, I. Levstik, R. Blinc, C. Filipic, J.Physique, 40, C3-303 (1979).
10. C.J. Böttcher, Theory of electric polarization, (Elsevier, Amsterdam, 1973).
11. M. Glogarova, L. Lejcek, J. Pavel, V. Janovec, J. Fousek, Mol.Cryst.Liq.Cryst., 91, 309 (1983).
12. Ph. Martinot-Lagarde, R. Duke, G. Durand, Mol.Cryst.Liq.Cryst., 75, 249 (1981).
13. Ph. Martinot-Lagarde, Mol.Cryst.Liq.Cryst., 66, 61 (1981).
14. A. Jákli, L. Bata, Á. Buka, N. Éber, I. Jánossy, J.Physique Lett., 46, L-759 (1985).
15. P. Pieranski, E. Guyon, P. Keller, J.Physique, 36, 1005 (1975).